Research on Engineering Structures & Materials
www.jresm.org
Research Group

Research Article

Shear behavior and failure mechanisms of steel fiber reinforced concrete beams incorporating silica fume: Experimental investigation with SEM–EDX based microstructural influence on structural response

Chakala Harsha Vardhan [*,1,a], Durga Chaitanya Kumar Jagarapu [1,b], D V S K Chaitanya [2,c], B.P.R.V.S.Priyatham [3,d], B Dileep Kumar Reddy [4,e]

[1]*Department of Civil Engineering, Koneru Lakshmaiah Education Foundation, Vaddeswaram, Guntur District, India*
[2]*Department of Civil Engineering, Acharya Nagarjuna University, Guntur District, India*
[3]*Department of Civil Engineering, GMR Institute of Technology (GMRIT) - Deemed to be University, Rajam, India*
[4]*Department of Civil Engineering, JNTUA College of Engineering, Pulivendula, YSR Kadapa District, India*

Article Info

Article History:

Received 06 Feb 2026

Accepted 26 Apr 2026

Keywords:

Shear behavior;
Fiber reinforced concrete;
Crack pattern;
Ductility;
Steel fibers;
Load-deflection response;
a/d ratio;
SEM-EDX analysis

Abstract

Shear failure in reinforced concrete beams is characterized by a sudden and brittle response posing significant risks to structural safety particularly in high-performance cementitious matrices. Although silica fume improves strength and durability it often reduces crack limit. This study addresses gap by establishing a direct equivalence between material-level interpretation and beam-scale shear behavior using concrete mixes containing 5% silica fume and steel fibers at volume fractions (V_f) of 0%, 0.75%, 1.0% and 1.25% were prepared among them 1.0% identified as optimum mix based on that an experimental program comprising cubes, cylinders and beam testing complemented by SEM-EDX microstructural analysis was conducted to investigate fiber-matrix interaction. Beam specimens were casted and tested under 4-point loading with a (a/d) ratio of 1.9 adapted limited transverse reinforcement to induce shear-critical behavior. Results indicate that RCSF0% fibers showed diagonal tension cracking leading to brittle shear failure within shear span. whereas, the RSCF1.0% mix demonstrated enhanced load capacity improved deformation resulting in a distinct shift from shear-dominated to flexure-controlled behavior. The findings further reveal that even with relatively larger stirrup spacing, steel fibers effectively bridged cracks at the microstructural level, enhancing shear resistance and improving the ductility and stability of the shear-critical structural members.

1. Introduction

Reinforced concrete beams are critical components in structural systems where shear resistance governs both safety and serviceability under increasing load demands unlike flexural behavior shear response is characterized by the rapid progression of inclined cracking & limited capacity of a shear redistribution once initiated shear cracking may propagate suddenly leading to abrupt failure with minimal warnings this behavior is particularly critical and structural number subjected

*Corresponding author: harsha01vardhan10@gmail.com
[a]orcid.org/ 0009-0009-1416-7569; [b]orcid.org/ 0000-0002-4497-0426; [c]orcid.org/0000-0002-6020-9215; [d]orcid.org/ 0000-0002-7032-0507; [e]orcid.org/ 0000-0001-6237-7899
DOI: http://dx.doi.org/10.17515/resm2026-1494me0206rs

to high shear to moment ratios where failure is governed by diagonal tension rather than material strength alone Consequently improving shear performance remains a central challenge in reinforced concrete designs [1]. Recent seismic events like Kahramanmaraş 2023 earthquake have magnitude of 7.8 highlighted the vulnerability of (R.C) members to brittle shear failures, inadequate shear capacity and poor detailing resulted in several structural damage and collapse [2, 20]. The adoption of high-performance concrete has further Intensified this challenge while such concrete provides enhanced compressive strength and durability, they often exhibit reduced deformation capacity under limited crack accommodation increased matrix stiffness accelerates crack localization especially under shear dominant Stress stages. As a result, high performance does not name necessarily translates into improved structural stability and in certain cases may increase susceptibility to brittle shear failure. This disconnects between strength enhancement and damage tolerance necessities additional mechanisms to Control cracking and sustain load transfer beyond matrix fracture. Silica fume is widely employed to improve concrete performance through pozzolanic reaction and microstructural densification the resulting refinement of pore structure enhances compressive strength and reduced permeability however this densification restricts Crack bridging and eliminates post crack deformation experimental observation indicates that silica fume modified concrete exhibits a reduced crack tolerance once Tensile stresses exceeder matrix capacity Under loading. The absence of intrinsic crack arrest mechanism leads to rapid stiffness degradation and unstable crack propagation under loading [14, 16]. Steel fibers provides a complementary mechanism by introducing distributed tensile resistance within the concrete matrix after cracking fibers bridge discontinuities Transfer stresses across crack plains and openings In shear critical games this action contributes to the preservation of aggregate interlocking and enhancements of double actions For longitudinal reinforcement rather than acting as a conventional reinforcement fiber modifies the crack process itself delays the crack localization and altering post cracking stiffness degradation the resulting response reflects a transition from little failure to ductile behavior. Furthermore, fiber has been shown to enhance seismic performance by improving confinement in structural members. The effectiveness of this mechanism depends on the fiber geometry volume of fraction dispersion and Interaction with the surrounding cementitious matrix of the concrete. Transverse reinforcement is required in concrete beams if shear demand is high and diagonal cracking cannot be resisted by concrete alone especially in beams with low shear span-to-depth ratios where brittle failure occurs [3, 6]. However, studies have shown that addition of fibers modifies the shear mechanism by enhancing aggregate interlocking and dowel action leading to more stable crack evolution compared to conventional beams [8, 15, 17]. This behavior has been further supported by theoretical models indicating fiber-induced tensile stress transfer contributes to an increase in shear capacity. Post-earthquake investigations consistently indicate that brittle shear failure and insufficient ductility are primary causes of structural damage in reinforced concrete members subjected to seismic loading. Field-based studies following 2023 Kahramanmaraş earthquake report that inadequate shear reinforcement and poor detailing [2, 10] led to rapid diagonal cracking at a degree range from 30-45° even compressive strength requirements were satisfied [13]. Fiber-reinforced concrete exhibit improved crack control and confinement, thereby enhancing seismic performance and delaying failure under cyclic loading conditions. Comparisons reveal that conventional concrete is highly susceptible to shear failure whereas fiber-modified concrete demonstrate improved deformation and structural capacity.

Microstructural investigations further support distinction by explaining the mechanisms governing crack investigation. SEM-based studies reveal that improved fiber-matrix formation enables stress transfer across interfaces through bridging action, thereby reducing crack growth EDX analysis confirms that interfacial adhesion and matrix densification significantly influence load transfer and arrest crack mechanism, resulting in unstable crack growth and rapid stiffness degradation. This evidence directly relates with structural observations, where fiber-reinforced concrete shows ductile response [8].

Steel fibers reduce crack opening by bridging inclined cracks and transferring tensile stresses after cracking, which delays crack growth and lowers the demand on stirrups by sharing shear resistance [4, 7, 21]. At higher fiber volume of fractions crack control improves initially however,

excessive fiber content may reduce workability and lead to non-uniform distribution, limiting effectiveness [5, 8, 22]. An increase in fiber aspect ratio improves crack-bridging and pull-out resistance, but very high aspect ratios can cause fiber balling and reduce overall efficiency in beams [9, 11].

Existing studies fiber-reinforced concrete often treats material properties and structural behavior separately with limited efforts to establish a direct link between microstructural characteristics and structural response. In addition, the combined influence of silica fume and steel fibers on shear behavior lacking, particularly due to the opposing effects of matrix densification. The study addresses gaps through an integrated experimental approach, to establish the relationship between material behavior and structural response. Initially, mechanical properties were evaluated for different (V_f) to identify optimum composition. then structural testing was conducted to access the response of the beams. SEM-EDX analysis performed to examine reaction of the supplementary cementitious (SCM) material and the fiber-matrix interaction governing post crack bridging. The novelty lies indirectly correlating material and microstructural behavior with the structural performance. The results demonstrate that fiber addition delays crack and improves the ductility even with the larger stirrup spacing in the structural element, thereby improving the reliability of shear-critical members.

2. Research Importance

This experimental investigation is important because it establishes a direct and systematic link between material-level optimization and shear behavior at the beam scale, which is often missing in existing studies. Most previous research adopts predefined fiber contents directly for beam testing or limits evaluation to material specimens without structural validation [3, 5, 7]. In the present work, the selection of steel fiber volume of fraction is conducted by compressive, stress-strain behavior tests performance before beam casting, ensuring that structural response reflects optimized material behavior. The experimental results compare steel fiber–reinforced concrete beams with conventional reinforced concrete beams by evaluating differences in load response, crack development and failure mode showing that fiber inclusion alters diagonal cracking behavior and promotes a more stable shear failure mechanism relative to brittle shear-dominated failure observed in normal beams [4, 8, 11].

3. Description of materials and specimens

3.1 Materials Properties

3.1.1 Cementitious Materials

Ordinary Portland Cement (OPC) of 53 grade was used as the primary binder. The cement complied with relevant Indian Standard specifications and had a specific gravity of 3.15. Silica fume was employed as a partial cement replacement to improve matrix densification and interfacial transition zone characteristics. Owing to its ultrafine particle size and high amorphous silica content, silica fume participates in pozzolanic reactions with calcium hydroxide to generate additional calcium silicate hydrate (C–S–H) gel. The specifications provided by the supplier are summarized in Table 1.

Table 1. Mineral admixture properties

Parameters	Specifications
Appearance	Grey powder
Bulk density at packing (kg/m^3)	588
Loss on ignition (%)	2.86
Specific gravity	2.29
Silica content by mass (%)	92.48
Moisture content (%)	0.31
Retained on 45 μm sieve (%)	6.28

3.1.2 Aggregates

Natural river sand was used as fine aggregate. The sand was clean, well graded and free from organic impurities, ensuring adequate workability and uniform fiber dispersion. All the materials are illustrated in (Fig. 1).

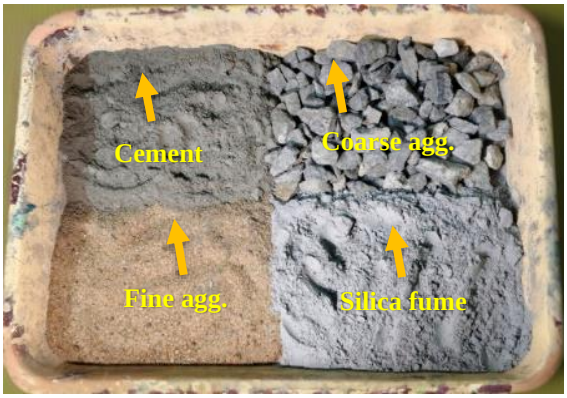

Fig. 1. Primary materials utilized in concrete mix preparation

Crushed angular coarse aggregate with a nominal maximum size of 20 mm was adopted to provide the primary load-bearing skeleton and improved mechanical interlock within the concrete matrix. As described in Table 2.

Table 2. Properties of aggregates employed in the experimental program

Property	Specific Gravity	Water Absorption (%)	Fineness Modulus	Nominal Size	Grading Zone
Fine Aggregate	2.65	1	2.70	4.75mm-90 µm	III
Coarse Aggregate	2.74	0.5	7.20	20 mm	—

3.1.3 Mixing Water

Potable water free from deleterious substances such as acids, alkalis, salts, and organic matter was used for both mixing and curing, in accordance with standard requirements for reinforced concrete.

3.1.4 Superplasticizer

A high-range water-reducing admixture (Hi-Forza 369) was incorporated to get required workability at a low w/c ratio particularly in mixes containing silica fume and steel fibers. The admixture was a yellowish-brown liquid with a specific gravity of 1.145 and pH of 6.8 indicating chemical blending with cementitious systems. The low chloride content 0.09% ensured that no adverse risk of reinforcement corrosion was introduced. The admixture acts as water reduction capacity of approximately 25% enabling improved flowability and cohesive behavior without segregation. A dosage of 1% by weight of binder was adopted to promote uniform fiber dispersion and consistent fresh-state performance.

3.1.5 Steel Reinforcement

High-yield deformed steel bars of grade Fe 550D were used as internal reinforcement. Longitudinal reinforcement consisted of 12 mm ϕ bars provided in both the top and bottom regions of the beam to resist flexural tension and compression. Transverse reinforcement was provided using 8 mm ϕ bars as stirrups to control shear cracking and confinement. All reinforcing bars satisfied the mechanical and ductility requirements. The supplier provided parameters are presented in Table 3.

Table 3. Reinforcement properties

Rebar size (ϕ)	Elastic modulus (GPa)	Density (g/cm³)	Shear strength (MPa)	Tensile strength (MPa)	Poisson's ratio
12mm, 8mm	200	7.85	319	550	0.30

3.1.6 Fibers

Hooked-end steel fibers were incorporated to enhance post-cracking behavior and shear resistance as shown in (Fig. 2). The hooked geometry improves mechanical anchorage and pull-out resistance, enabling effective crack bridging under tensile stress. Fibers were added at specified volume of fractions (V_f).

Fig. 2. Representative steel fiber materials utilized in the experimental program

To study their influence on crack development and failure mode in reinforced concrete beams. The properties of the fibers were offered by the material supplier shown in Table 4.

Table 4. Summary of fiber properties

Property	Value
Length (mm)	35
Aspect Ratio	46.6
Density (g/cm³)	7.8
Tensile Strength (MPa)	1150
Shape	Hooked-end

3.1.7 Concrete Mix Design

Concrete mixes for RCSF0% and RCSF1.0% means (reinforced concrete steel fiber beams) were designed as per IS:456-2000 and IS:10262-2019 [25, 26] for M50 grade using 5% silica fume and a PCE-based superplasticizer based on mechanical performance, RCSF1.0% was selected for beam casting along with the control mix. The mix design parameters are shown in Table 5.

Table 5. Mix design proportions adopted for experimental concrete specimens

Mix	Cement (kg/m³)	Silica fume (kg/m³)	Fine aggregate (kg/m³)	Coarse aggregate (kg/m³)	Super plasticizer (kg/m³)	Steel fibers (kg/m³)	Water (kg/m³)
RCSF0%	410	22	735	1182	4.31	0	138
RCSF1.0%	410	22	735	1182	4.31	78	138

4. Experimental Investigation

4.1 Mechanical Properties

The RCSF0% mix showed a slump of 106 mm, while the RCSF1.0% mix recorded 72 mm, indicating reduced workability due to fiber addition. Cube and cylinder specimens were cured for 28 days prior to testing. Compressive, stress-strain behavior tests were conducted in accordance with relevant IS codes, using the specified loading rates for each test to ensure consistent and reliable mechanical performance evaluation. Below (Fig. 3) shows the test setups of the specimens.

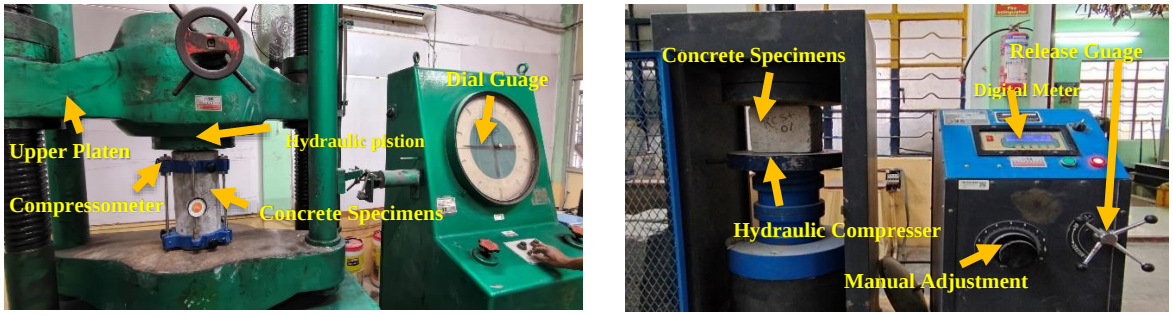

Fig. 3. Experimental test setup of compression testing machine for concrete specimens

4.2 Flexural Studies of Fiber Reinforced Concrete Beams

Four reinforced concrete beams were casted to evaluate load–deflection behaviour. Each beam had the dimensions of 1.5m ×0.23m ×0.30m. The specimens were categorized into two groups:

- Conventional Control Beam (RCSF0%)

Two reinforced concrete beams were cast using M50 grade concrete with 5% silica fume as a partial replacement for cement and conventional steel reinforcement bars.

- Fiber Reinforced Concrete Beam (RCSF1.0%)

Two fiber reinforced concrete beams (FRC) were casted using M50 grade concrete and conventional steel reinforcement with 1.0% steel fibers incorporated to enhance post-cracking and shear performance. Four beams were cured for 28 days using the wet gunny bag method before structural testing.

4.3 Detailing of Reinforcement and Beam Fabrication

The beams were reinforced to ensure adequate resistance against flexural and shear actions. Longitudinal reinforcement Ø of 12 mm bars was provided in both the tension and compression zones to resist tensile stresses and maintain flexural stability. To control shear stresses, 8 mm Ø transverse reinforcement was provided @ 230 mm c/c spacing using Fe550D grade steel. This comparatively wider spacing was intentionally adopted to limit the contribution of stirrups and enable clearer assessment of the influence of steel fibers on shear resistance and crack control. For the steel fiber–reinforced beams, hooked-end steel fibers were incorporated by (V_f) into the concrete matrix to supplement shear resistance through crack bridging and post-cracking stress transfer. (Fig. 4) illustrates the typical reinforcement layout adopted for all test specimens.

Beam moulds with internal dimensions of (1.5m×0.23m×0.30m) were overly cleaned and inspected to ensure rigidity before a thin layer of form release oil was applied. The reinforcement was placed inside the mould with suitable cover blocks to maintain clear cover at the bottom and sides. Concrete was mixed corresponding to the quantified mixes and placed into the mould in 3 layers. Each layer was compacted using a mechanical vibrator to expel entrapped air and ensure uniform integration. The top surface was finished and specimens were left undisturbed for 24 h before demolding. Subsequently, beams were cured using wet gunny bags to promote strength development and control hydration heat. As illustrated in (Fig. 5).

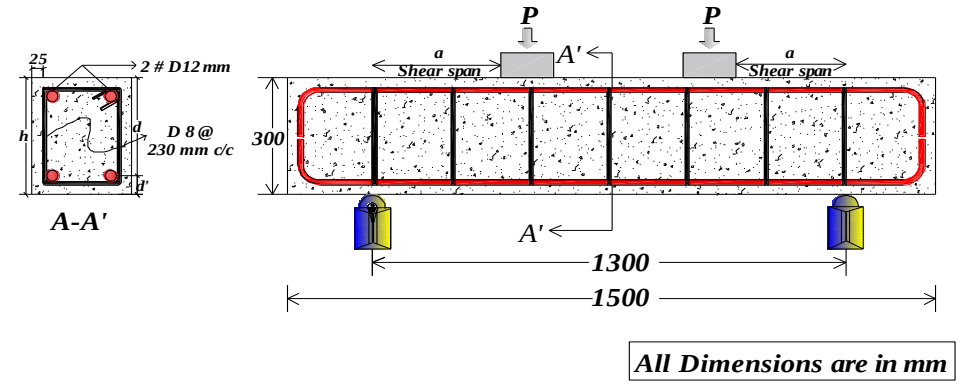

(a)

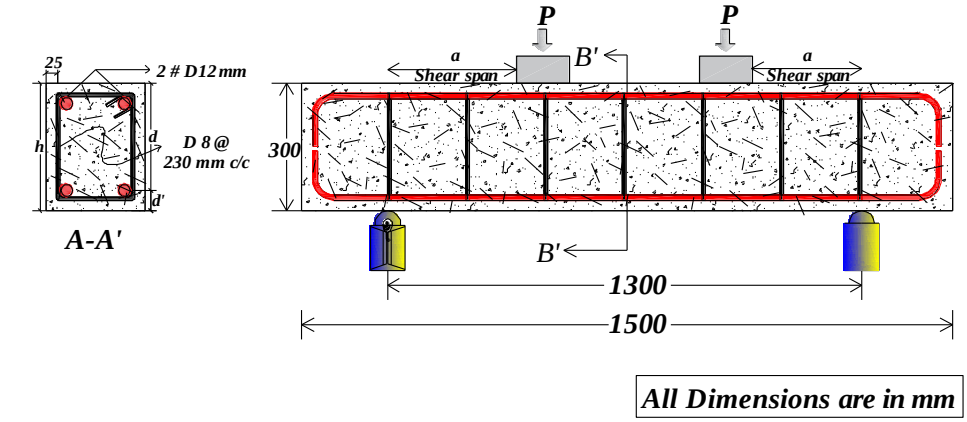

(b)

(c)

Fig. 4. Reinforcement configuration of tested beams shown in real and schematic forms A) RCSF0% B) RCSF1.0% C) Demonstrates actual reinforcement configuration

Fig. 5. Membarane curing of R.C.C Beams

4.4 Test Setup of the Beam

After completion of curing, beam specimens were tested in a calibrated 200T capacity loading frame under four-point loading to examine shear behavior of simply supported members. One end of each beam was supported on a hinge and the other on a roller to allow free rotation and longitudinal movement. A linear variable differential transducer (LVDT) was positioned at mid-span to continuously record vertical deflection during loading as displayed in (Fig. 6). Prior to testing, reference grid lines were marked at 100 mm intervals along the beam length to facilitate identification and monitoring of crack initiation and propagation. Load was applied incrementally until failure and the resulting load–deflection data were used to assess stiffness response, cracking behavior and shear and flexural performance of the beams.

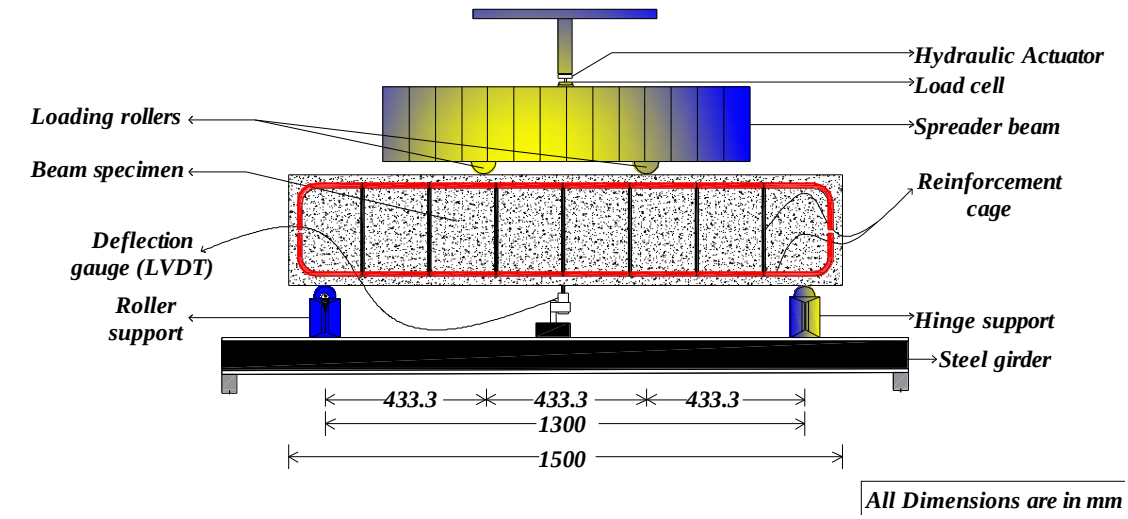

Fig. 6. Schematic representation of experimental test configuration

5. Results and Discussion

5.1 Mechanical Properties of Concrete

Cube and cylinder specimens corresponding to each concrete mix were tested at 7 and 28 days to examine strength development and deformation characteristics. The cube compressive strength for mixes with varying (V_f) {0%, 0.75%, 1.0%, 1.25%} among them RCSF1.0% mix attained 59.12 N/mm^2 at 28 days, whereas the control mix RCSF0% exhibited a comparatively lower value of 52.60 N/mm^2, while mixes 0.75%, 1.25% achieved 55.72 N/mm^2, 58.30 N/mm^2 respectively shown in (Fig. 7). The strength reduction in 1.25% is attributed due to reduced workability and fiber agglomeration, which leads to non-uniform dispersion and weakens the matrix continuity. Therefore 1.0% was selected for casting cylinders and beams to evaluate stress-strain behavior and structural performance of the beam [4, 12, 17, 24].

The strength of RCSF0% remained limited by the brittle nature of the cement matrix, where confined tensile microcracking governs the appearance of crushing (Fig. 8) highlights the failure modes of cube and cylinder specimens with crack propagation paths drawn and emphasized in yellow. (Fig. 9), illustrates the compressive stress–strain responses of the RCSF0% and RCSF1.0% concretes at 7 and 28 days revealing a pronounced influence of steel fiber incorporation on deformation behavior. All mixes exhibited an initially linear elastic segment. However, fiber addition vaguely increased the strain equivalent to peak stress.

The control mix reached maximum stress at a similarly lower strain and undergone post-peak reduction indicative of brittle matrix crushing and unstable crack growth. Similarly, (FRC) mixtures produced a larger nonlinear zone and maintained critical stress beyond peak, indicating fiber pull-out mechanisms and crack-bridging progressive debonding. The most progressive post-peak response and the best strain capacity were consistently achieved by the RCSF1.0% fiber mix. Peak stress was mostly influenced by age but ductility ranking unchanged confirming the role of fibers in promoting ductile response and enhanced energy dissipation.

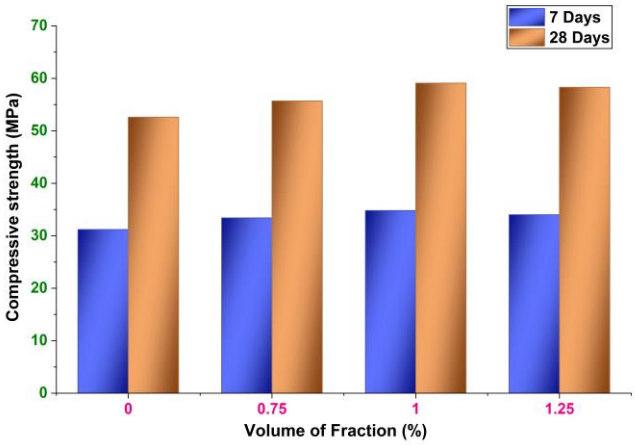

Fig. 7. Variation in compressive strength of concrete cubes with respect to curing age

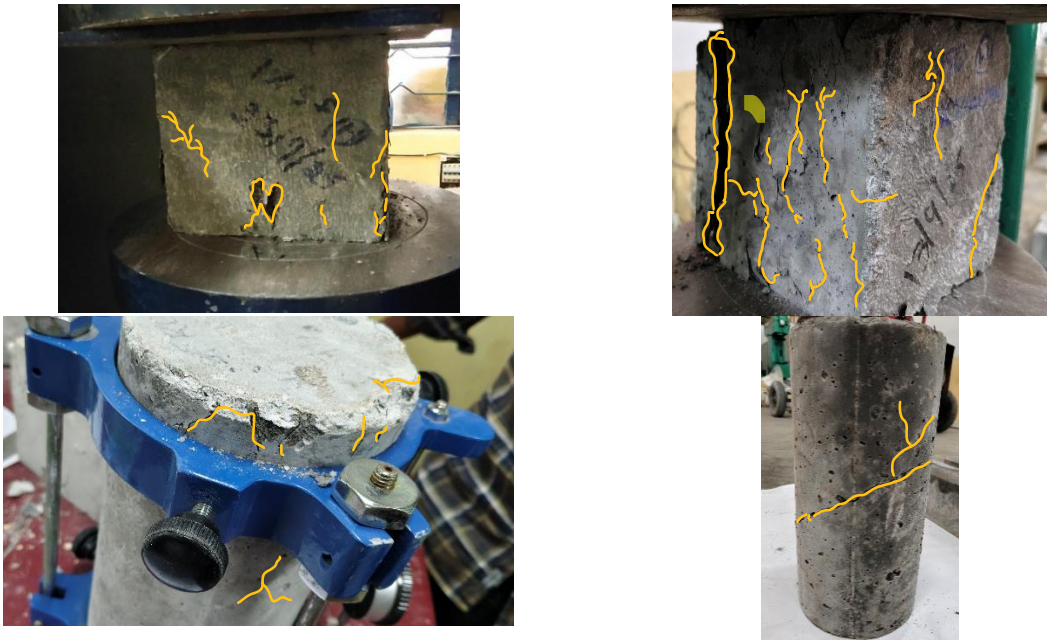

Fig. 8. Depicts the crack pattern developed in concrete specimen

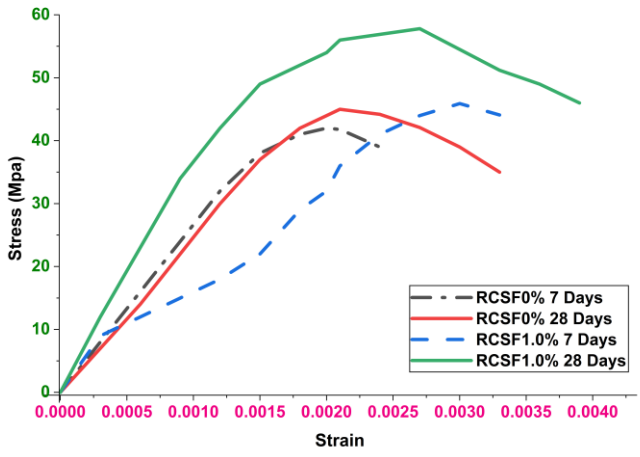

Fig. 9. Stress–strain behavior of a concrete

5.2 Structural Response and Damage Evolution of RC Beams

Flexural testing of reinforced concrete beams was carried out to quantify the influence of steel fiber incorporation on the load–deflection response *P–Δ*, crack initiation and propagation characteristics, stiffness degradation $K = P/\Delta$, and governing failure mode. For each concrete mix, two beam specimens were tested under identical four-point loading conditions with $a/d = 1.9$ and all specimens were detailed with transverse reinforcement @230 mm c/c spacing to ensure consistent shear confinement. In this study, the structural responses are based on the average behavior of the two specimens for each mix, and all results discussed herein correspond to these averaged values [27]. The representative average load–deflection responses *P–Δ* for all mixes are summarized in Table 6, thereby providing a reliable basis for subsequent analysis of stiffness degradation, energy absorption $E = \int P\, d\Delta$ and ductility index $\mu = \Delta u/\Delta y$. Particular emphasis was placed on the ability of steel fibers to delay first cracking P_{cr}, restrict crack opening *(w)* and modify the post-cracking response through crack-bridging and stress redistribution mechanisms [19].

Table 6. Average ultimate load and variability of tested RC beams

Mix	P_u (kN)	Standard deviation (kN)	Coefficient of variation (%)
RCSF0%	204.8	2.26	1.1
RCSF1.0%	246.0	3.39	1.4

The control beams without fibers (RCSF0%) attained an average ultimate load of $P_u = 204.8$ kN with a corresponding maximum midspan deflection of $\Delta_u = 19.1$ mm, whereas the RCSF1.0% mix achieved a higher average ultimate load of $P_u = 246.0$ kN and a larger ultimate deflection of $\Delta_u = 29.2$ mm, as shown in (Fig. 10). The comparatively large deflections observed in both beam series are mainly attributed to the wide stirrup spacing of 230 mm c/c, which reduced the direct contribution of transverse reinforcement to shear resistance and permitted greater shear deformation prior to failure.

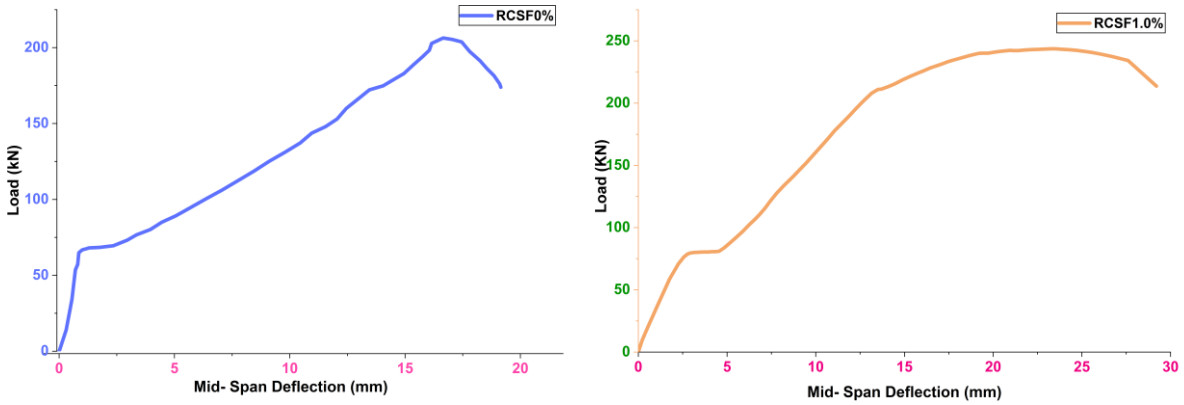

Fig. 10. Load vs deflection response of beam specimens under loading

The ultimate shear capacity may be expressed as $V_u = V_c + V_s + V_f$, where V_c - the concrete contribution, V_s- stirrup contribution, and V_f- fiber contribution. In RCSF0% beams, the absence of fibers limited shear transfer to $V_c$and V_s, leading to early diagonal cracking and restricted post-cracking stiffness, thereby constraining deformation capacity [23]. In contrast, RCSF1.0% beams benefited from the additional fiber-bridging component V_f, which enhanced aggregate interlock, restrained crack opening, and improved stress redistribution, allowing higher loads to be sustained with stable deformation. At ultimate load, all beams exhibited an average end rotation of approximately $\theta \approx 3°$. The predominance of shear failure in RCSF0% beams and flexure-controlled failure in RCSF1.0% beams confirms that steel fibers effectively compensated for the reduced stirrup contribution, increased deformation capacity, and promoted a more ductile, flexure-governed response.

5.2.1 Comparison of the Conventional Beam and Fiber Reinforced Beam

The control beams exhibited early diagonal cracking followed by brittle shear failure, whereas the (FRC) beams developed well-distributed flexural cracks with delayed crack propagation and gradual stiffness degradation. Higher ultimate load and improved post-cracking deformation capacity were consistently observed in RCSF1.0% specimens. The contrast in cracking pattern, load–deflection response and failure mode between the two beam types is illustrated in (Fig 11).

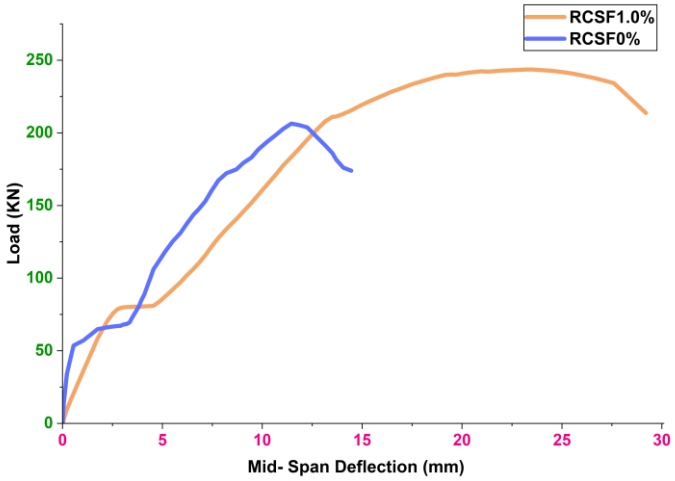

Fig. 11. Comparative assessment of load-deflection characteristics of beam specimens

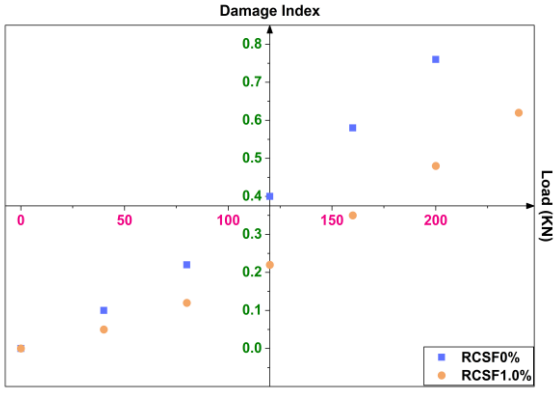

(a)

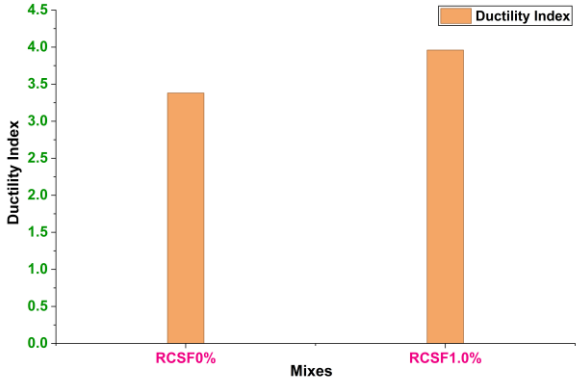

(b)

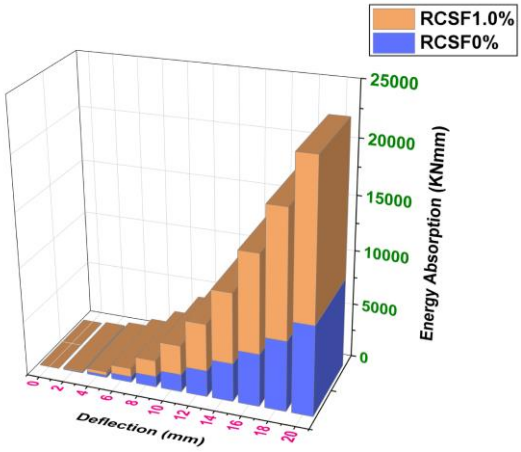

(c)

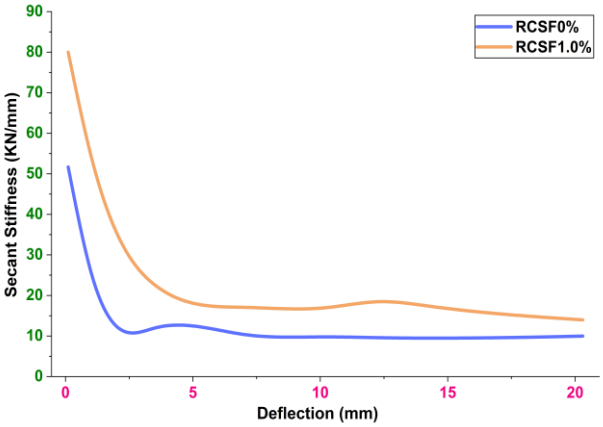

(d)

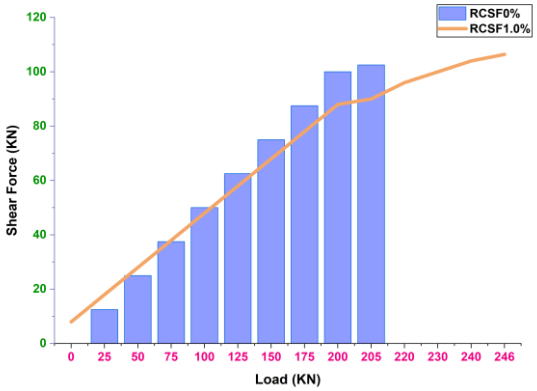

(e)

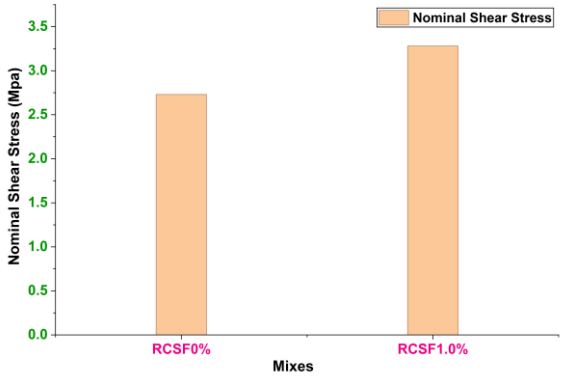

(f)

Fig. 12. Comparative evaluation of (a) Damage index (b) Ductility index (c) Energy absorption (d) Secant stiffness degradation (e) Shear force and (f) Nominal shear stress of beam specimens.

Control beams exhibited rapid stiffness reduction after the onset of diagonal cracking subsequently weak load transfer and leads to shear failure. In contrast, RCSF1.0% beams maintained higher load levels with progressive deformation indicating that fiber bridging across developing cracks maintained tensile stress transfer after matrix cracking. The presence of fibers restricted crack opening and delayed crack coalescence allowing stresses to be redistributed within the tension zone and across inclined crack planes. This mechanism explains the higher ultimate load and shifting failure pattern from shear zone failure behavior to flexure-controlled behavior in RCSF1.0% beams. The variation of secant stiffness degradation with deflection is shown in (Fig. 12). Stiffness evolution with increasing deflection, expressed through the secant stiffness degradation confirms that (FRC) beams retain greater load-carrying capability at comparable deformation levels.

$$K = P/\Delta \tag{1}$$

Reduced stiffness loss in RCSF1.0% beams is associated with controlled microcrack growth and gradual fiber pull-out, whereas RCSF0% beams experience rapid stiffness decay due to unstable diagonal cracking. The larger ductility index recorded for RCSF1.0% beams reflect the ability of fibers to sustain load beyond first cracking and accommodate inelastic deformation prior to failure. A comparison of ductility damage for both beam types is shown in (Fig. 12). Similarly, the higher cumulative energy absorption observed in (FRC) beams results from repeated crack bridging and frictional pull-out of fibers. The cumulative energy absorption trends, which dissipate energy during crack propagation. Damage index is evaluated using, progressed steadily in RCSF1.0% beams, indicating delayed stiffness degradation and distributed cracking.

$$D = 1 - (K/K_0) \tag{2}$$

The evolution of the damage index with applied load further confirms a slower accumulation of damage in the F.R.C beams. In addition, the load–shear force response obtained from $V = P/2$ indicate improved shear resistance for the RCSF1.0% mix. The ultimate shear capacity of the RCSF1.0% beams increased by approximately, compared with the control beams. These observations collectively confirm that steel fibers enhance crack stability, improve deformation capacity and transform the overall response toward a more stable and ductile structural behavior.

$$\frac{V_{u,\mathrm{SFRC}} - V_{u,\mathrm{RC}}}{V_{u,\mathrm{RC}}} \times 100 \approx 20\% \tag{3}$$

5.3 Structural Distress Modes

The crack patterns shown in (Fig. 13) highlights the governing role of steel fibers in controlling shear transfer, crack evolution and failure mode. The RCSF0% beams exhibited shear-dominated

behavior characterized by the formation of a major diagonal tension crack within the shear span, initiating near the support and propagating toward the loading point.

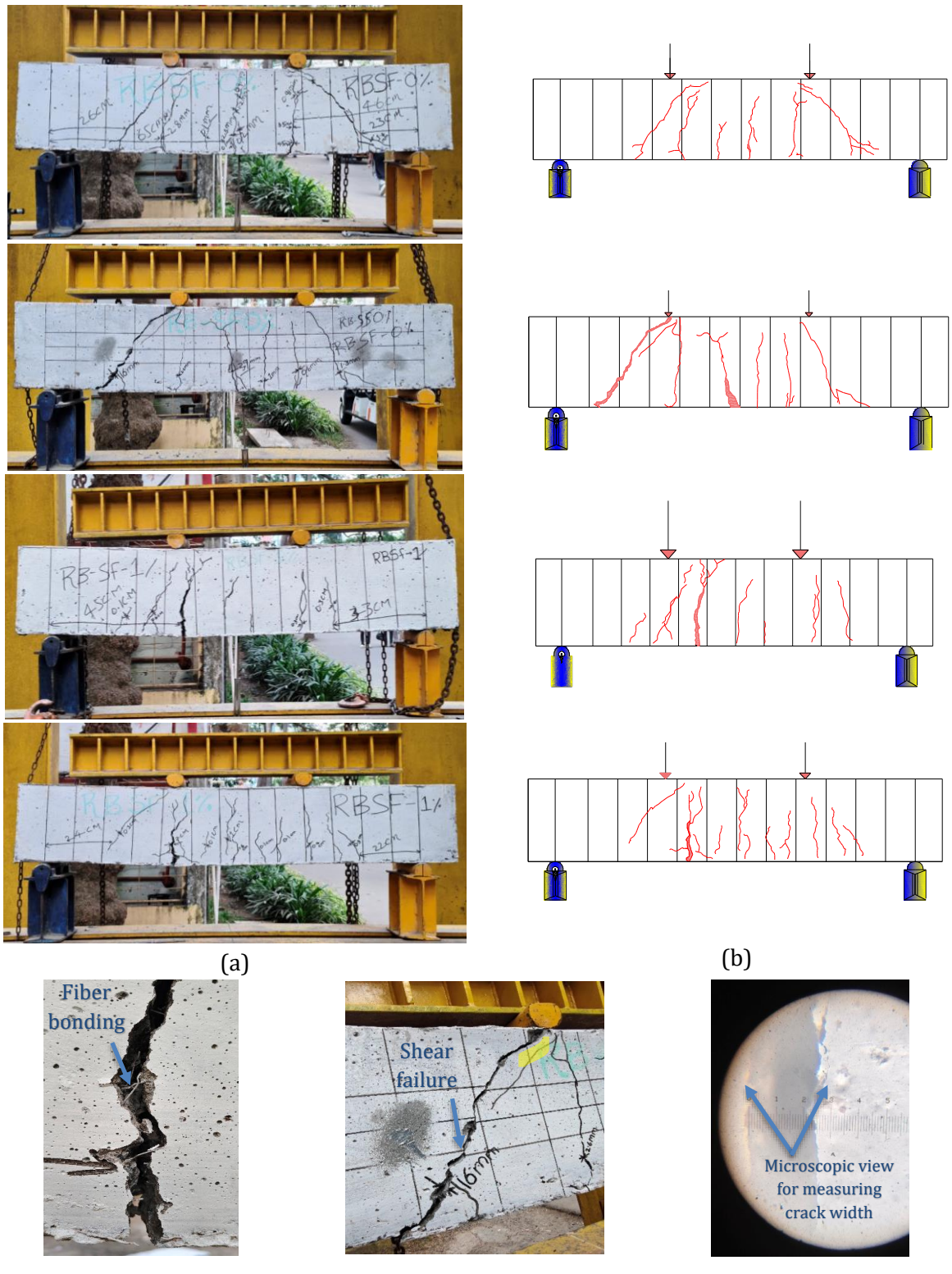

Fig. 13. Representation of crack development through (A) From experimental testing and (B) Schematic representation of crack mechanism

The average diagonal crack width was approximately 8.25 mm at a distance of about 295 mm from the support with the help of microscope, while only limited flexural cracking developed in the constant moment region with an average maximum width of about 2.6 mm. The presence of web-shear and shear-compression cracks near the compression zone indicates crushing of the diagonal

concrete strut and severe concentration of principal tensile stress (σ_1), leading to brittle shear failure with limited post-cracking stress redistribution.

In contrast, RCSF1.0% beams displayed initial fine, closely spaced vertical flexural cracks followed by flexural–shear cracks forming at approximately 450 mm from the supports, with an average maximum width of about 4.3 mm and no web-shear cracks were observed. Steel fibers allow crack-bridging action, enhancing aggregate interlock and dowel action enabling sustained tensile stress transfer across cracked planes. This mechanism increased the post-cracking tensile benefaction of concrete and the effective shear resistance, thereby reducing the nominal shear stress ratio relative to the cracking inception (Fig. 12). Consequently, cracking progressed in a stable and distributed manner, stiffness degradation was gradual and failure shifted from brittle shear in RCSF0% beams to a ductile, flexure-controlled mechanism in RCSF1.0% beams.

$$\tau_v = \frac{V}{bd} \tag{4}$$

5.4 SEM EDX analysis

The SEM analysis (Fig. 14) reveals a distinct difference in the microstructural organization of RCSF0% and RCSF1.0% concrete mixes. In RCSF0%, the matrix is mainly composed of C–S–H gel integrated with plate-like calcium hydroxide and occasional unhydrated clinker particles, indicating a dense but heterogeneous paste. Although the incorporation of 5% silica fume refines the pore structure through secondary pozzolanic reactions, the absence of fibers permits microcracks to propagate preferentially along weak paste regions and interfacial transition zones (ITZ), resulting in limited crack arrest capability and a brittle shear-governed response. Thus, shear resistance in RCSF0% is primarily led by matrix strength and aggregate interlock, which are insufficient to maintain post-cracking load transfer.

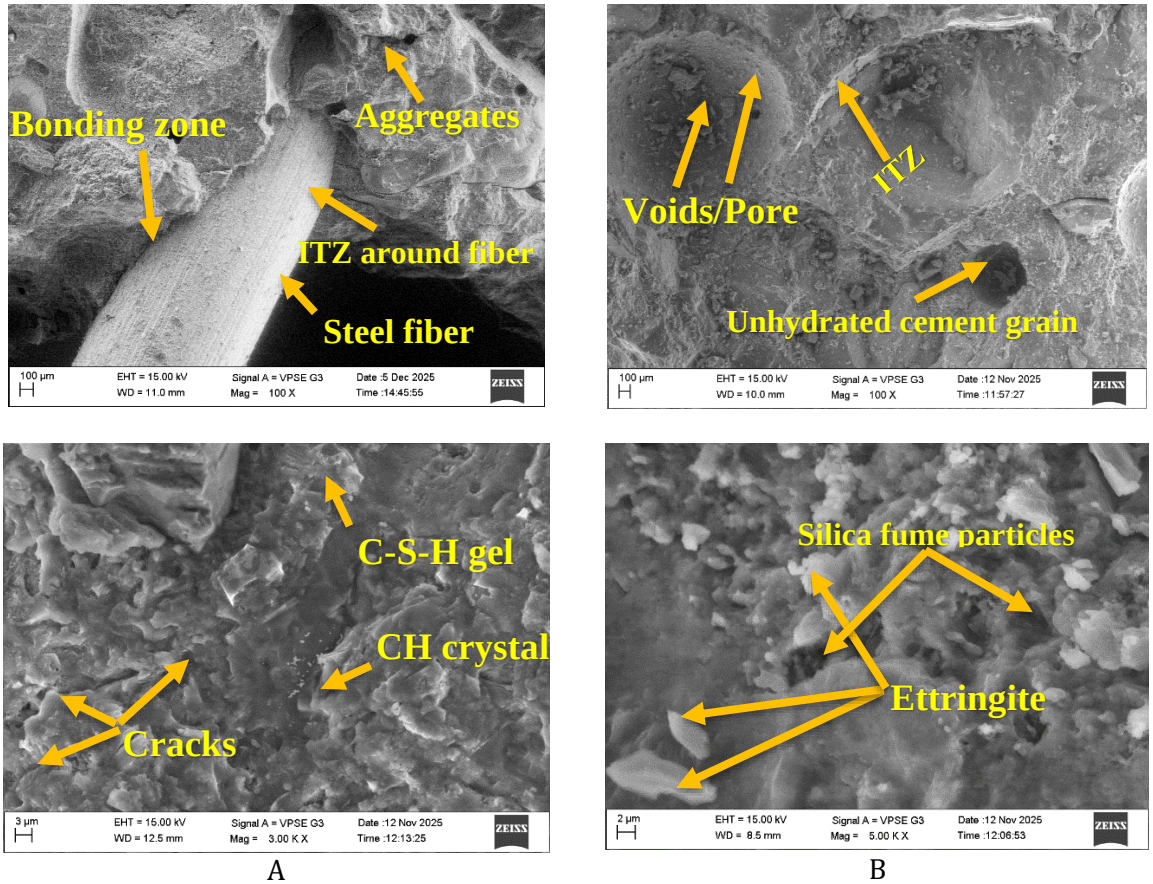

A B

Fig. 14. SEM images comparasion of A) FRC and B) Nominal concrete

In contrast, the RCSF1.0% mix exhibits a well-developed fiber–matrix interface, where hydration products are tightly adhered to the steel fiber surface forming a compact and continuous ITZ. The

rough fiber texture promotes mechanical interlocking at the same time, the surrounding C–S–H layer enhances chemical bonding enabling efficient stress transfer between the matrix and fibers. Under shear loading, fibers bridge developing diagonal cracks, restrict crack widening and provide additional shear resistance through pull-out and debonding mechanisms. In (Fig. 15) EDX results showing dominant Ca (26.9 wt.%) and O (52.3 wt.%) with measurable Si and Al confirm a hydration product-rich matrix with Ca-rich zones that further strengthen the fiber–matrix bond. The combined effect of matrix densification and effective fiber bridging explains the higher load-carrying capacity, improved post-cracking stiffness and limited ductile shear behavior of the RCSF1.0% mix compared to the brittle response of RCSF0%. The enhanced fiber–matrix interaction promotes crack bridging, increased post-peak load resistance and higher energy absorption, thereby transforming the failure mode from brittle to ductile failure.

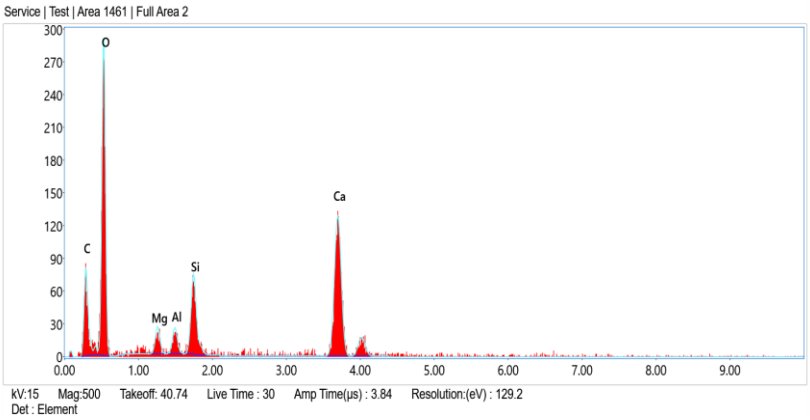

Fig. 15. EDX analysis indicating elemental distribution of the concrete

5.5 Limitations and Validations of The Study

The present investigation is based on a controlled experimental program with a limited number of beam specimens and two beam-level mixes (0% and 1.0%). Although an optimum fiber content was identified through preliminary testing considering fiber (V_f) {0%, 0.75%, 1.0%, 1.25%}, only a single optimized fraction (1.0%) was considered for structural evaluation and a full parametric study at the beam level was not undertaken. Therefore, the results should be interpreted as indicative rather than statistically generalized. In addition, the distribution and orientation of fibers within the concrete matrix may vary due to workability constraints, which can influence local stress transfer and crack propagation behavior. The experimental program was limited to monotonic loading conditions and the response under cyclic or seismic loading was not investigated. Furthermore, the specimens represent laboratory-scale elements and scale effects may influence the behavior of full-scale structural members. The study is also limited to experimental observations without incorporating numerical or analytical modelling, which could further enhance the generalization of the results.

The validity of the present findings is supported through comparison with established experimental and analytical studies. A comparative evaluation with previous studies indicates that the observed 20% increase in shear capacity aligns withs findings reported by [4, 8], while enhanced ductility and delayed crack observed in this study exceed those reported in conventional SFRC beams it confirms the synergistic effect of silica fume and steel fibers improves the shear resistance were shown in Table 7. Fiber-reinforced concrete enhanced shear strength delayed crack initiation and improved deformation capacity. This behavior is attributed to crack-bridging action of fibers to sustains tensile stress transfer across inclined cracks and also preventing premature shear failure. SEM observations further substantiate this mechanism revealing strong fiber-matrix bonding. This micro-to-macro interaction governs the improved structural response. Results indicate that fiber bridging compensates for reduced transverse reinforcement, thereby lowering the dependency on the closely spaced stirrups it enhances ductility in the structural elements

Table 7. Comparative evaluation of shear behavior and failure mechanisms of FRC beams with existing studies

Study	Fiber Content (%)	Approach	Shear Behavior	Failure Mode Transition	Key Mechanism	Comparison with Present Study
Yuan et al. [4]	1.0	Experimental	Increased shear capacity	Shear → Flexure	Demonstrated fiber effectiveness in shear strengthening	Present study shows higher improvement due to silica fume synergy
Dinh et al. [8]	0.75–1.5	Analytical + Experimental	Improved shear resistance	Controlled shear cracking	Developed analytical shear models for SFRC beams	Present study experimentally validates similar trends with microstructural evidence
Yoo and Yang [18]	1.0	Experimental	Enhanced ductility	Distributed cracking	Established enhanced ductility and energy absorption	Present study Confirms ductility enhancement with additional SEM-EDX validation
De Resende et al. [12]	1.0	Experimental	Improved dowel action	Reduced crack width	Highlighted reduction in crack width and improved shear transfer	Present study shows improved crack control with stronger fiber-matrix bonding
Thurimella et al. [24]	0-1.25	Experimental + microstructural	Improved capacity of load and crack control	Ductile behavior	Fiber bridging and enhanced bonding between fibers	Prior research emphasized flexural behavior; this study explores shear behavior showing ductility with SEM-EDX validation
Present Study	1.0	Experimental + SEM–EDX	Significant improvement	Shear → Flexure	Establishes micro-to-macro correlation using SEM-EDX	Demonstrates superior performance and validates mechanism of the materials experimentally

6. Conclusion

The study examined shear behavior of fiber-reinforced concrete beam through an integrated experimental approach linking material behavior, structural response and microstructural mechanisms to understand role of steel fibers under shear-critical conditions.

- RCSF0% revealed a slump of 106 mm, whereas RCSF1.0% showed 72 mm showed reduced workability due to increased surface area & mechanical interlocking of fibers restrict free flow and increase internal friction within the fresh matrix. The compressive strength of concrete increased from RCSF0% mix 52.60 N/mm^2 to 59.12 N/mm^2 RCSF1.0% mix improved concrete matrix densification from silica fume and uniform stress redistribution caused by fiber bridging delays microcrack fusion under compression. However, fiber content beyond 1.0% was found

to reduce strength due to fiber agglomeration and reduced workability confirming 1.0% as optimum fiber dosage.

- Stress–strain curves demonstrated enhanced ductility for RCSF1.0%, presented by extended post-peak deformation, whereas RCSF0% showed a higher dropping in strength reflecting brittle matrix cracking and limited energy dissipation capacity.
- The RCSF1.0% beams developed higher load capacity, larger deformation, and greater rotation 3° with less cracks demonstrating that steel fibers effectively controlled crack growth and sustained tensile stress after cracking. In contrast, the control beams RCSF0% showed lower rotation 2° extensive shear cracking and early stiffness loss reflecting brittle shear-dominated behavior because absence of fibers.
- Despite stirrups spaced at 230 mm c/c RCSF1.0% beams failed in flexure, while RCSF0% beams exhibited shear-dominated brittle failure. In RCSF0% mix, principal tensile stresses (σ_1) along inclined shear planes exceeded concrete tensile capacity forming dominant diagonal cracks. In RCSF1.0% mix fibers reduced tensile stress concentration by bridging inclined cracks changes load distribution mechanism from shear to flexure failure zone.
- Addition of fibers in RCSF1.0% beams provide an effective internal shear-resisting mechanism through crack-bridging action and showed steadier stiffness degradation, higher ductility index, greater cumulative energy absorption and reduced damage index progression verifying that fiber pull-out delay stiffness loss and distribute damage more uniformly.
- The addition (V_f) of 1.0% fibers increased the nominal shear stress from 2.73 MPa to 3.28 MPa and the ultimate shear force from 102.40 kN to 123.00 kN equivalent to an improvement of approximately 20% in shear capacity primarily due to effective fiber bridging and improved post-cracking stress transfer. The reduced damage index and increased ductility index ($\mu_{RC} \approx 3.4$, $\mu_{SFRC} \approx 4.0$) of the SFRC beams indicate delayed stiffness degradation and a transition from brittle shear-dominated behavior to a more stable and ductile response.
- Further studies should examine aspect ratio of fiber contents, geometry and hybrid reinforcement strategies through extended experimental programs, including full-scale structural members such as beam-column joints and frames. In addition, behaviour under cyclic and seismic loading with different reinforcement configuration by varying the spacing to examine role of fibers and also analyze failure progression. The development of validated numerical models is essential to simulate crack evaluation and fiber interaction, enabling parametric studies and supporting interaction of fiber-based shear reinforcement into design-oriented guidelines.

References

[1] Alhilali SS, Ali HK, Shubber MA. Experimental investigation on structural shear behaviour and mechanical characteristics of steel fiber reinforced concrete beams without stirrups. Mathematical Modelling and Engineering Problems, 2025;12(3):884–892. https://doi.org/10.18280/mmep.120314

[2] Işık E, Shao Y, Hadzima-Nyarko M, Radu D, Bulajic B, Lozancic S. Enhancing the seismic safety of upgraded RC buildings using FRP retrofitting: analytical and field evidence from the 2023 Kahramanmaraş earthquakes. Bulletin of Earthquake Engineering. 2025;24(3):1467–1501. https://doi.org/10.1007/s10518-025-02338-zzzz

[3] Hamoodi AZ, Alhussein TH, Zewair MS, Naser KZ. Experimental study for the effect of steel fibers types and volume fraction on the flexural performance of RC beams. Mathematical Modelling and Engineering Problems, 2025;12(7):2203–2215. https://doi.org/10.18280/mmep.120701

[4] Yuan T, Yoo D, Yang J, Yoon Y. Shear capacity contribution of steel fiber reinforced high-strength concrete compared with and without stirrup. International Journal of Concrete Structures and Materials, 2020;14(1). https://doi.org/10.1186/s40069-020-0396-2

[5] Kara IF, Dundar C. Prediction of deflection of high strength steel fiber reinforced concrete beams and columns. Computers and Concrete, 2012;9(2):133–151. https://doi.org/10.12989/cac.2012.9.2.133

[6] Imam M, Vandewalle L, Mortelmans F. Shear–moment analysis of reinforced high strength concrete beams containing steel fibers. Canadian Journal of Civil Engineering, 1995;22(3):462–470. https://doi.org/10.1139/l95-054

[7] Torres JA, Lantsoght EOD. Influence of fiber content on shear capacity of steel fiber-reinforced concrete beams. Fibers, 2019;7(12):102. https://doi.org/10.3390/fib7120102

[8] Dinh HH, Parra-Montesinos GJ, Wight JK. Shear strength model for steel fiber reinforced concrete beams without stirrup reinforcement. Journal of Structural Engineering, 2010;137(10):1039–1051. https://doi.org/10.1061/(asce)st.1943-541x.0000362
[9] Słowik M. Shear failure mechanism in concrete beams. Procedia Materials Science, 2014;3:1977–1982. https://doi.org/10.1016/j.mspro.2014.06.318
[10] Işık E, Radu D, Harirchian E, Avcil F, Arkan E, Büyüksaraç A, Hadzima-Nyarko M. Failures in reinforced-concrete columns and proposals for reinforcement solutions: insights from the 2023 Kahramanmaraş earthquakes. Buildings. 2025;15(9):1535. https://doi.org/10.3390/buildings15091535
[11] Abdul-Zaher AS, Abdul-Hafez LM, Tawfic YR, Hammed O. Shear behavior of fiber reinforced concrete beams. Journal of Engineering Sciences, 2016;44(2):132–144. https://doi.org/10.21608/jesaun.2016.117592
[12] De Resende TL, Cardoso DCT, Shehata LCD. Influence of steel fibers on the dowel action of RC beams without stirrups. Engineering Structures, 2020;221:111044. https://doi.org/10.1016/j.engstruct.2020.111044
[13] Ozmen HB, Inel M. Effect of concrete strength and detailing properties on seismic damage for RC structures. Research & Design. 2024;1(1):1–11. https://doi.org/10.17515/rede2024-005en1124rs
[14] Abdullatif NW, Alhayani AA. Shear and flexural strength of pumice lightweight concrete beams with silica fume. Research on Engineering Structures and Materials. 2025. https://doi.org/10.17515/resm2025-971me0703rs
[15] Khuntia M, Stojadinovic B, Goel SC. Shear strength of normal and high-strength fiber reinforced concrete beams without stirrups. ACI Structural Journal, 1999;96(2). https://doi.org/10.14359/620
[16] Kytinou VK, Chalioris CE, Karayannis CG, Elenas A. Effect of steel fibers on the hysteretic performance of concrete beams with steel reinforcement—tests and analysis. Materials, 2020;13(13):2923. https://doi.org/10.3390/ma13132923
[17] Hamoodi AZ. Shear behavior of fiber-reinforced concrete beams: an experimental study. International Journal of Geomate, 2021;21(86). https://doi.org/10.21660/2021.86.j2263
[18] Yoo D, Yang J. Effects of stirrup, steel fiber, and beam size on shear behavior of high-strength concrete beams. Cement and Concrete Composites, 2017;87:137–148. https://doi.org/10.1016/j.cemconcomp.2017.12.010
[19] Hasgul U, Yavas A, Birol T, Turker K. Steel fiber use as shear reinforcement on I-shaped UHP-FRC beams. Applied Sciences, 2019;9(24):5526. https://doi.org/10.3390/app9245526
[20] Singh SS, Kumar A, Mishra LK, Ghosh G. Impact of fiber on the confinement of beam and column members towards seismic performance of RC building. Journal of Building Pathology and Rehabilitation. 2025;10(1). https://doi.org/10.1007/s41024-025-00589-6
[21] Muneam AK, Makki RF. Shear capacity of reinforced concrete beams with recycled steel fibers. Open Engineering, 2023;13(1). https://doi.org/10.1515/eng-2022-0457
[22] Sanal I. Effect of shear span-to-depth ratio on mechanical performance and cracking behavior of high strength steel fiber-reinforced concrete beams without conventional reinforcement. Mechanics of Advanced Materials and Structures, 2019;27(21):1849–1864. https://doi.org/10.1080/15376494.2018.1527963
[23] Ma K, Ma Y, Liu B. Experimental investigation on ultra high performance fiber reinforced concrete beams. Mechanics of Advanced Materials and Structures, 2022;30(6):1155–1171. https://doi.org/10.1080/15376494.2022.2028947
[24] Thurimella MK, J BCK, N L, A GFR, Singh RK. Experimental investigation of structural behaviour and microstructural characteristics of steel fibre-reinforced concrete beams. Australian Journal of Structural Engineering. 2026:1–17. https://doi.org/10.1080/13287982.2026.2643532
[25] Bureau of Indian Standards. Plain and reinforced concrete—Code of practice (IS 456:2000). New Delhi, India: BIS, 2000.
[26] Bureau of Indian Standards. Concrete mix proportioning—Guidelines (IS 10262:2019). New Delhi, India: BIS, 2019.
[27] Bureau of Indian Standards. Ductile detailing of reinforced concrete structures subjected to seismic forces (IS 13920:2016). New Delhi, India: BIS; 2016.